

RESEARCH ARTICLE

## Cytotoxicity evaluation of synthesized silver nanoparticles by a Green method against ovarian cancer cell lines

Shahla Abbasi<sup>1</sup>, Ahmet İlhan<sup>2</sup>, Hadi Jabbari<sup>3</sup>, Parisa Javidzade<sup>4</sup>, Maede Safari<sup>5</sup>, Firoozeh Abolhasani Zadeh<sup>6\*</sup>

<sup>1</sup> Gynecologist, Department of medical Education, Kosar hospital, Broujerd, Lorestan, Iran

<sup>2</sup> Department of Medical Biochemistry, Faculty of Medicine, Cukurova University, Adana, Turkey

<sup>3</sup> Department of Chemistry, Payame Noor University, P.O. Box 19395-4697 Tehran, Iran

<sup>4</sup> Department of Genetics, Faculty of Science, Shahid Chamran University of Ahvaz, Ahvaz, Iran

<sup>5</sup> Department of Urology, Isfahan University of Medical Sciences, Isfahan, Iran

<sup>6</sup> Department of Surgery, Faculty of Medicine, Kerman University of Medical Sciences, Kerman, Iran

### ARTICLE INFO

#### Article History:

Received 27 January 2022

Accepted 02 April 2022

Published 01 May 2022

#### Keywords:

Silver nanoparticle  
(Ag-NPs)  
*Malva sylvestris* L  
Biosynthesis  
Ovarian cancer

### ABSTRACT

**Objective(s):** In recent years, the attention of many was focused on the features of the Green Synthesis process, such as its simplicity, cost-effectiveness, and environmental friendliness. This study investigates the feasibility of manufacturing silver nanoparticles from *Malva sylvestris* L aqueous extract and evaluates its anti-cancer effect on ovarian cancer cell lines OVCAR-3 and SK-OV-3.

**Methods:** The aqueous extract of *Malva sylvestris* L proved to be capable of synthesizing silver nanoparticles (Ag-NPs) and the success of the procedure was affirmed through the results of characterizing analyzes such as UV-Vis spectroscopy, transmission electron microscopy (TEM), and dynamic light scattering (DLS). Additionally, we assessed the anti-cancer impacts of synthesized Ag-NPs on OVCAR-3 and SK-OV-3 cell lines by the means of MTT assay. The Bax, Bcl-2, caspase 3, and caspase 8 expression at mRNA levels were also estimated using real-time PCR.

**Results:** The appearance of an absorption peak at 462 nm using a spectrophotometer signified the complete synthesis of silver nanoparticles. The electron microscope images showed that the nanoparticles were spherical and had an average size of about 74.4 nm. Ag-NPs at the concentration (10-200nM) inhibited the proliferation of OVCAR-3 and SK-OV-3 cell lines. Moreover, treatment resulted in down-regulating Bcl-2 while up-regulating Bax and caspase 3 and caspase 8 expression.

**Conclusions:** In this study, synthesized Ag-NPs using *Malva sylvestris* L could induce a robust anti-cancer effect on ovarian cells in vitro by improving Bax/Bcl-2 ratio and triggering the apoptosis pathway.

### How to cite this article

Abbasi Sh., İlhan A., Jabbari H., Javidzade P., Safari M., Abolhasani Zadeh F. Cytotoxicity evaluation of synthesized silver nanoparticles by a Green method against ovarian cancer cell lines. *Nanomed Res J*, 2022; 7(2): 156-164. DOI: 10.22034/nmrj.2022.02.005

### INTRODUCTION

Nanoparticles (NPs) implicate a notable range of materials in the sizes of below 100 nm and due to their varying properties, they can be employed in multiple implementations including

medical, pharmaceutical, manufacturing and materials, environmental, electronics, energy collection, and mechanical industries. Carbon nanotubes, quantum dots, nanorods, nanocapsules, nanoemulsions, fullerenes, metallic NPs, ceramic NPs, and polymer NPs are among the different

\* Corresponding Author Email: [Firoozeh1981@gmail.com](mailto:Firoozeh1981@gmail.com)

types of nanoparticles [1-3] that contain unique features such as conductivity, stability, catalytic, and antibacterial capabilities. Cancer is known as the most stressful and life-threatening disease with the highest worldwide rates of mortality due to the advent of multiple drug resistance and the progress of severe adverse consequences by various chemotherapies. To address this issue, therapeutic approaches for early cancer diagnosis and treatment with low side effects are urgently needed. Nano-oncology research has resulted in creating a variety of nanoscale materials, technologies, and therapeutic agents to provide early diagnosis and effective treatment for cancer [4, 5]. AgNPs could reduce cancer cells viability and cause membrane leakage in a dose-dependent manner. AgNPs are capable of boosting the generation of reactive oxygen species and hydroxyl radicals in cells, while their apoptotic effects were further confirmed by caspase 3 activation and DNA nuclear fragmentation. The cytotoxic and apoptotic properties of these nanoparticles signifies the role of produced reactive oxygen species by AgNPs throughout the process of apoptosis[6].

The fascinating qualities of metallic NPs triggered the design of different synthesizing methodologies. However, the synthesized silver (Ag) NPs by various physical and chemical techniques implicate the exertion of hazardous chemicals and their products are neither economically feasible nor environmentally friendly [7-9]. Considering the limited available time for finding practical solutions to this obstacle, green chemistry stands as a applicable substitute for environmentally harmful methods and products that pose severe hazardous impacts on the world[10-12]. The novel premises of 'Green Nanotechnology' can cause tremendous impacts on the industrial revolution. Furtive extractions from natural precursors have resulted in the development of biogenic resources to fabricate advanced nanomaterials in a cost-effective and straightforward process[13, 14]. An effective biogenic mechanism can be the economical and green solution to environmental obstacles by highly decreasing the exertion of harmful reagents through the application of cheap natural and waste products and produce value-added nanomaterials with extensive relevance. Many different biological agents, similar to bacteria, fungi, plant extracts, etc., can be employed to perform the green synthesis of metal nanoparticles due to their biocompatibility. The reduction of

dissolved metals ions into nano-metals can be facilitated by the bio-agents of a green process[15, 16]. The topic of nanoparticles biosynthesis attracted the focus of many due to the exceeding demand for the design of environmentally benign technologies in the field of materials synthesis. As an example, Mousavi and colleagues used *Artemisia turcomanica* leaf extract to synthesize silver nanoparticles and investigated its anti-cancer activity in gastric cancer cell lines (AGS). In contrast to untreated cells, the results showed increased apoptosis in cells treated with biological silver nanoparticles ( $p < .001$ ). In conformity to the collected data, it was concluded that biologically produced silver nanoparticles triggered apoptosis and had a dose- and time-dependent cytotoxic and anti-cancer effect on gastric cancer cell lines. Commercial silver nanoparticles may not have the same anti-cancer capabilities as biologically produced nanoparticles[17]. *Malva sylvestris L* (in the family *Malvaceae*) is recognized by about 40 taxa around the world, which is an annual herb native to Europe, North Africa, and South-west Asia with the appearance of shallowly lobed leaves and purple flowers that bloom in late spring. *M. sylvestris L.* is exerted as a healing treatment for burn and dermal infected wounds, bronchitis, and inflammations, as well as digestive difficulties such as constipation [18, 19]. It is consisted of various metabolites including phenols, flavonoids, esters, and peptides that are capable of mediating the synthesis of nanoparticles[20]. This work presented the synthesis of silver nanoparticle through a green strategy with the usage of *M. sylvestris L* extract in mild conditions. Aqueous *M. sylvestris L* solution can facilitate a secured, cheap, and environmental-friendly procedure for the green synthesis of Ag NPs in water media. In the following, we distinguished the obtained product through the results of certain physical methods, and also investigated the cytotoxic impacts of biologically synthesized AgNPs on ovarian cancer cells.

## MATERIALS AND METHODS

### Materials

AgNO<sub>3</sub> (CAS-Nr.: 7761-88-8) as a source of silver ions was purchased from Merck (Germany). MTT reagents and mRNA Isolation Kit were purchased from Gibco (Germany). Further, the High Capacity cDNA Reverse Transcription Kit was attained from Thermo Scientific (USA). In addition, the nuclease-free water was purchased

from Invitrogen™ (Germany), and SYBR Premix Ex Taq kit was also procured from TAKARA (Japan).

#### *Characterizations of silver nanoparticles*

Transmission electron microscopy (TEM) analysis was performed by the application of a (CM30 3000Kv) to characterize the morphology and size of the nanoparticles. Dynamic light scattering (DLS) analysis was conducted as a complementary TEM through a computerized inspection system (MALVERN Zen3600) supplied with DTS® (nano) software to characterize the average size distribution of nanoparticles. A varian Cary 50 UV-vis spectrophotometer was employed to complete the UVVis spectroscopy analyses that involved the recording of Spectra in a range of 300-700 nm.

#### *Preparation of aqueous extract of Malva sylvestris L plant*

About 3 grams of the dried plant was boiled in 10 ml of deionized water for 15 minutes at 100 °C to be positioned on a shaker for the duration of 24 hours. The extract was cleansed for two rounds subsequent to being centrifuged(1000 rpm,30 min).

#### *Green synthesis of silver particles by the aqueous extract of Malva sylvestris L plant*

6 ml of 0.02 mM silver nitrate solution was appended to 4 ml of aqueous extract of *Malva sylvestris L* and placed on a magnetic stirrer for 12 hours at room temperature. About 20 minutes after the interaction, a color alteration was observed in the solution, turning from light yellow to dark brown, which indicated the synthesis of silver NPs.

#### *Cell culture*

We cultured ovarian cancer cells, OVCAR-3 and SK-OV-3 (ATCC), in Dulbecco's Modified Eagle's Medium (DMEM) supplemented with fetal bovine serum (FBS) 10%. Also, 100 units/ml of penicillin and 100 µg/ml of streptomycin (PAA, Austria) were added to culture media for the purpose of inhibiting the bacterial contamination of cell cultures, since they can display efficient combined activities toward gram-positive and gram-negative bacteria. In the following, the cells were kept in humidified air with 5% CO<sub>2</sub> at 37 °C.

#### *MTT assay*

The cytotoxicity of AgNPs against SK-OV-3

and OVCAR-3 was evaluated through the results of MTT assay. Initially, we seeded SK-OV-3 and OVCAR-3 cells in 96-well plates at a density of 5×10<sup>4</sup> cells per well. Thereafter, we treated the SK-OV-3 and OVCAR-3 cells with 0-200 nM concentrations of AgNPs within 12-72 hours of treatment. Subsequent to appending 20 µL of 5 mg MTT/ml medium to the SK-OV-3 and OVCAR-3 cells that accompanied wells, they were stored at 37°C for the duration of 4 hours and the OD of the well was estimated by the application of ELISA reader at the wavelength of 570 nm.

#### *RNA Isolation*

The total RNA of SK-OV-3 and OVCAR-3 cells was isolated by using the mRNA Isolation Kit (Gibco, Germany). Moreover, the quality and abundance of isolated RNA content were determined by the exertion of Nanodrop-2000.

#### *Reverse transcription and cDNA synthesis*

The transcription of isolated total RNA into cDNA was completed by the means of High Capacity cDNA Reverse Transcription Kit (RevertAid First Strand cDNA Synthesis Kit, Thermo Scientific, USA). In brief, the mixture of nuclease-free water (Invitrogen™, Germany) and a concentration of 10 µL was added to the 1 µg mixture of RNA with random hexamer primer (1 µL). Once the tubes were positioned in a thermocycler at 65 °C for 5 minutes, every box was retained on ice to complete the appending of other reagents as the last step. The First-strand cDNA was amplified under the conditions of 5 minutes at 25 °C, 60 minutes at 42 °C, and 5 minutes at 70 °C.

#### *Real Time-PCR*

StepOnePlus Real-Time PCR system (Applied Biosystems, USA) and an SYBR Premix Ex Taq kit (TAKARA, Japan) are needed to accomplish real-time PCR. In this step, a standard reaction mixture (20 µl) was mixed with 10 µl of SYBR Premix Ex Taq 2x, 1 µl of template cDNA, 5 µl of ultra-pure water, and 200 nM volumes of primers.

Table 1 exhibits the applied primer sequences in real-time PCR, while GAPDH was exerted in the form of internal control. All of the tests were completed in triplicate in regard to each data point.

#### *Statistical Analysis*

The data of statistical analysis was gathered through the utilization of GraphPad Prism version

Table 1. Primer pairs used for Real-time PCR

Gene		Primer Sequence (5'-3')
Bax	F	TTTGCTTCAGGGTTTCATCC
	R	GCCACTCGGAAAAAGACCTC
Bcl-2	F	GGATTGTGGCCTTCTTTGAG
	R	CAGCCAGGAGAAATCAAACAG
Caspase 3	F	TGAGCCATGGTGAAGAAGGA
	R	TCGGCTCCACTGGTATTTT
Caspase 8	F	CAGGCAGGGCTCAAATTTCT
	R	TCTGCTCACTTCTTGAAATCTGA
GAPDH	F	GAGTCAACGGATTGGTTCGT
	R	TTGATTTTGGAGGGATCTCG

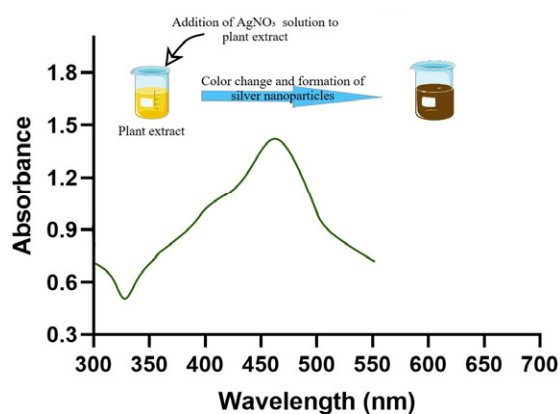


Fig. 1. UV-vis spectroscopy of Ag NPs

8.01. The consequences were represented as means  $\pm$  SEM from three independent tests using the Student's t-test. The P-value  $<0.05$  was expressed as statistically significant.

## RESULT AND DISCUSSION

### UV-Vis spectroscopy analysis

As a result of adding silver nitrate to the plant extract, a color alteration was observed from light yellow to dark brown. This observation indicated the completion of silver nanoparticles synthesizing procedure and is related to the surface plasmon resonance, size, and form of the obtained product. In harmony to Fig. 1, the detected sharp peak near 462 nm affirmed the successful synthesis of silver nanoparticles. Based on other researches, the observed bond correlates to colloidal silver nanosphere absorption in the 450-500 nm range[21].

### TEM and DLS investigation

Considering Fig. 2, the TEM images of silver nanoparticles displayed their spherical morphology. The average size of nanoparticles was about 74.4 nanometers, and the size distribution of nanoparticles was in the range of 24.08 to 178.31 nanometers. The particle size distribution histogram for nanoparticles generated using the DLS approach is shown in Fig. 3. In conformity to the tests results, the obtained nanoparticles contained an average size of 179 nm. The results of DLS and TEM do not coincide. DLS examines the hydrodynamic diameter of nanoparticles and their surrounding cover, which explains the difference. Furthermore, the attachment of some nanoparticles to one another, which leads to the formation of aggregations, is quiet conceivable throughout an aqueous environment. DLS measurements were conducted in the following to

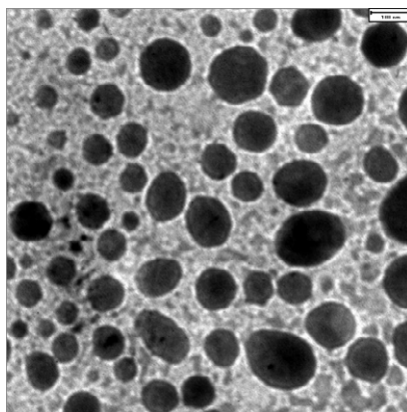


Fig. 2. TEM image of silver NPs

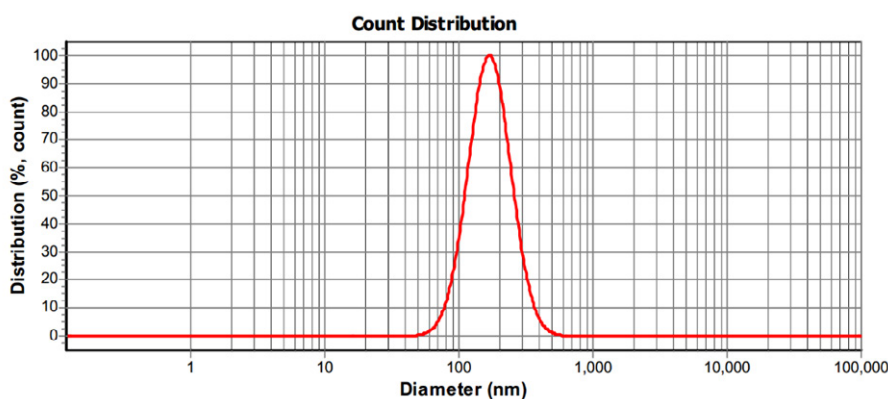


Fig. 3. DLS of green synthesized silver NPs

obtain the total diameter of collected nanoparticles. The particle size distribution of nanoparticles referred to a highly narrow to an extensive range in DLS, depending on the size of nanoparticles and the magnitude of biological components associated with diverse plant extract nanoparticles. Similar studies were reported on this disparity in particle size distribution as well [2].

*Ag-NPs stimulated cytotoxicity toward SK-OV-3 and OVCAR-3 cell lines*

Concerning the MTT assay results, 10, 20, 50, 100, 150, and 200 nM of AgNPs concentration abrogated the viability of SK-OV-3 and OVCAR-3 cell lines after being exposed for 12-72 hours ( $P < 0.05$ ) (Fig. 4A, B). Based on consequences, the suppressive impacts of AgNPs on cell viability relied on the applied time and dosage ( $P < 0.05$ ) (Fig. 4A, B). The IC<sub>50</sub> values of AgNPs in SK-OV-3 and OVCAR-3 cell lines are listed in Table 2.

The attained RESULTS of our study were consistent with the outcomes of other associated reports. Meanwhile, studies have indicated that AgNP could provoke strong cytotoxicity in vitro versus human colon cancer HT29 cells [22]. Further, AgNPs (median 30.71 nm size) abrogated the survival of liver carcinoma cells with 75 µg/mL of the IC<sub>50</sub> value [23]. AgNP also could strongly reduce the viability of A549 lung carcinoma cells mainly via promoting the levels of reactive oxygen species (ROS) [24]. Importantly, it was also suggested that the thermophilic fungus *Humicola* sp can be used for the biosynthesis of AgNPs [25]. Synthesized AgNPs elicited cytotoxicity versus NIH3T3 mouse embryonic fibroblast cell line and MDA-MB-231 cell line in vitro [25]. In addition, Boca et al. (2014) designed folic acid-conjugated, SERS-labeled silver nanotriangles for multimodal recognition and targeted photothermal therapy on human ovarian cancer cells [26].

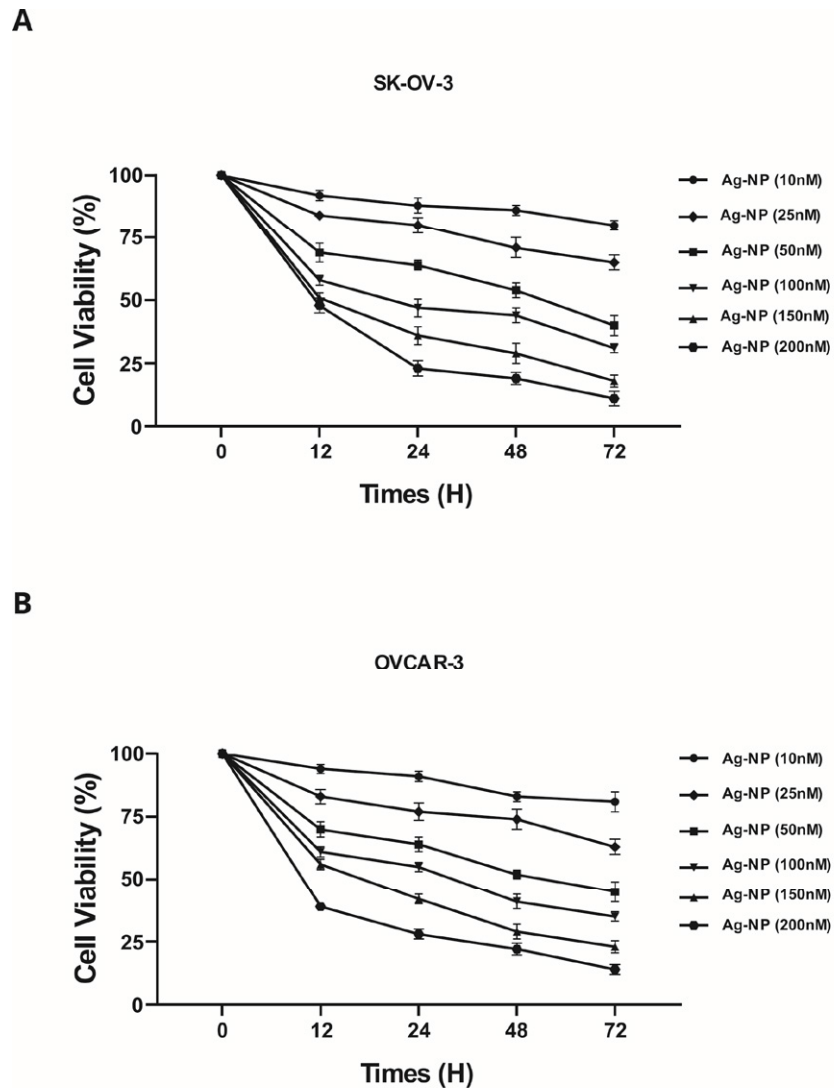


Fig. 4. MTT assay consequences based on the AgNPs effect on SK-OV-3 (A) and OVCAR-3 cell lines viability (B) in the course of 12, 24, 48, and 72 hours of treatment. Three independent examinations are included in the presented data. All of the values are expressed in mean  $\pm$  SEM.

Table 2. AgNPs IC50 value (Mean $\pm$ SEM) ( $\mu$ g/ml)

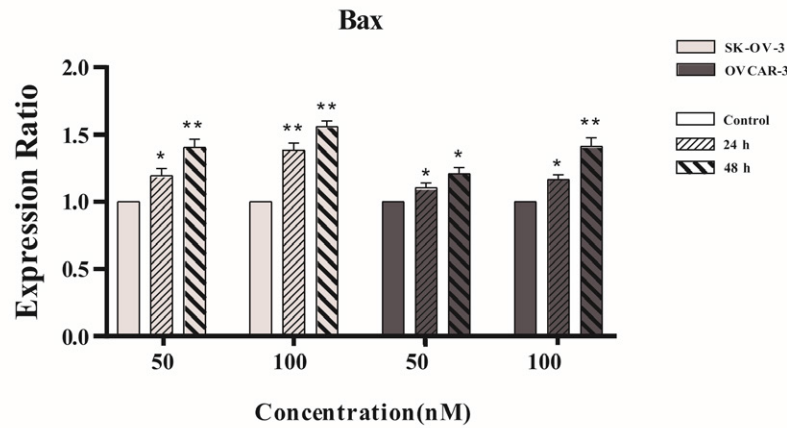
Cell line	IC50 value (12 h)	IC50 value (24 h)	IC50 value (48 h)	IC50 value (72 h)
SK-OV-3	171.34 $\pm$ 4.26 nM	94.98 $\pm$ 3.19 nM	72.23 $\pm$ 3.71 nM	36.09 $\pm$ 2.43 nM
OVCAR-3	163.14 $\pm$ 3.27 nM	124.23 $\pm$ 3.78 nM	64.56 $\pm$ 3.78 nM	48.7 $\pm$ 2.96 nM

*AgNPs enhanced Bax/Bcl-2 expression ratio*

We assessed the mRNA levels of pro-apoptotic proteins Bax and Bcl-2 by the application of real-time PCR in SK-OV-3 and OVCAR-3 cell lines

subsequent to being treated with 50 and 100 nM of AgNPs for 24 and 48 hours (Fig. 5A, B). Accordingly, AgNPs 50 and 100 nM improved the expression levels of Bax in both SK-OV-3 and

A



B

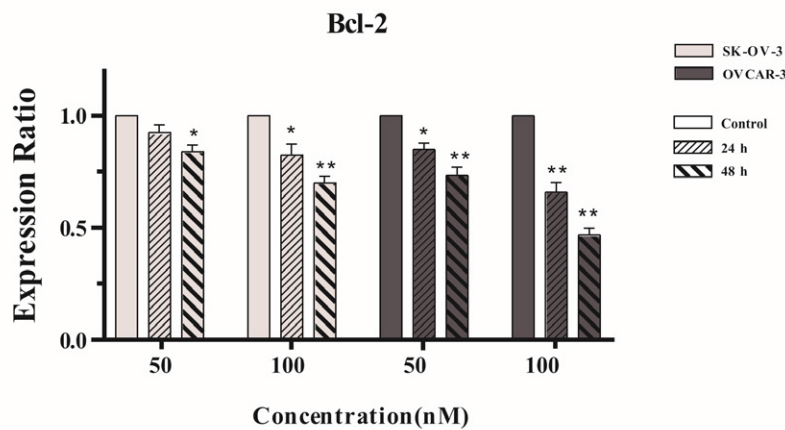


Fig. 5. The real time-PCR outcomes of Bax (A) and Bcl-2 (B) expression in SK-OV-3 and OVCAR-3 cell lines. Data is exhibited as means  $\pm$ SEM from three individual tests. GAPDH acted as the internal control. The Student's t-test was applied to configure the observed statistical differences. P values <0.05 were noted as statistically significant. (\* ;  $p < 0.05$ , \*\* ;  $p < 0.01$ )

OVCAR-3 cell lines at 24 and 48 hours of treatment ( $P < 0.05$ ) (Fig. 5A). The Bax expression was observed more clearly in the case of SK-OV-3 cell lines (Fig. 5A) when compared to that of OVCAR-3 cell lines. The analysis also showed that AgNPs 50 and 100 nM down-regulated the expression levels of Bcl-2 in both SK-OV-3 and OVCAR-3 cell lines ( $P < 0.05$ ) (Fig. 5B). In comparison to the outcomes of SK-OV-3, this reduction was more evident in OVCAR-3 cell lines (Fig. 5B).

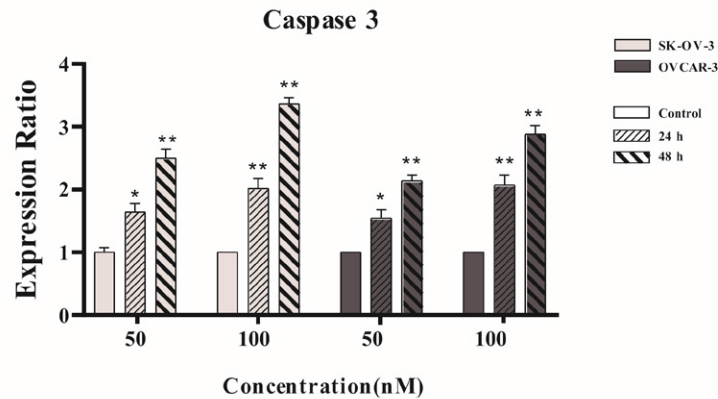
A myriad of studies has indicated that AgNPs could improve Bax expression leading to reduced viability and impaired apoptosis in cancer cells [27, 28]. In this light, *Achillea biebersteinii* flower extract-based biosynthesized AgNPs induced

cytotoxicity versus breast cancer cells by up-regulating Bax expression [29]. In addition, AgNPs improved Bax/Bcl-2 expression ratio leading to tumor cell eradication in vitro and in vivo [30, 31]. Similarly, Zhang et al. exhibited that AgNPs resulted in attenuation in Bcl-2 expression levels in cancer cells [32].

#### AgNPs improved caspase 3 and 8 expression

The exertion of Real-time PCR was considered to perform an assessment on the mRNA levels of caspase 3 and caspase 8 in SK-OV-3 and OVCAR-3 cell lines subsequent to being exposed to 50 and 100 nM of AgNPs throughout 24 and 48 hours of treatment (Fig. 6A, B). Considering the

A



B

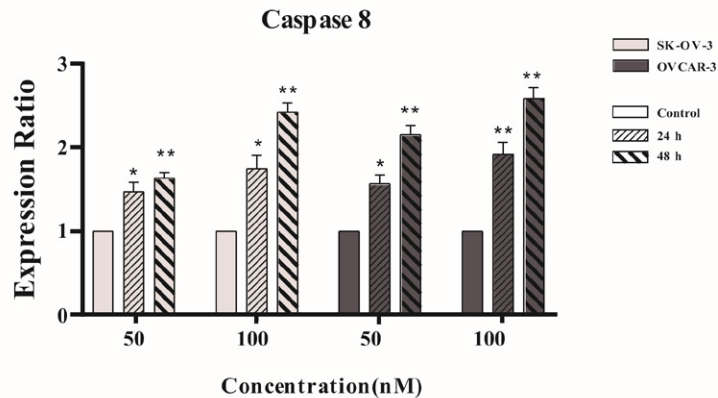


Fig. 6. The real time-PCR outcomes of caspase 3 (A) and caspase 8 (B) expression in SK-OV-3 and OVCAR-3 cell lines. Data is exhibited as means  $\pm$ SEM from three individual tests. GAPDH functioned as the internal control. The Student's t-test was applied to configure the observed statistical differences. P values <0.05 were noted as statistically significant. (\* ; p < 0.05, \*\* ; p < 0.01)

consequences, 50 and 100 nM of AgNPs strongly up-regulated the expression levels of both caspases in both SK-OV-3 and OVCAR-3 cell lines (P<0.05) (Fig. 6A, B).

In 2020, Singh et al. reported the biosynthesis and configuration of AgNPs by the application of papaya leaf extract (PLE). The established AgNPs induced robust apoptosis in human prostate (DU145) cancer cells mainly by up-regulating caspase 3 expression [28]. Likewise, AgNPs synthesized using *Artemisia oliveriana* extract were able to induce apoptosis in the A549 cell line mainly by improving caspase 3 and caspase 9 expression [33].

#### CONCLUSION

Green nanoparticle synthesis is an ecofriendly,

easy, and cost-effective way for avoiding the problems that chemical synthesis causes. *Malva sylvestris L* aqueous extracts were utilized as the reducing agent in this research to reduce Ag<sup>+</sup> cation. As a result of the AgNO<sub>3</sub> reaction in the presence of *Malva sylvestris L* aqueous extracts, silver nanoparticles were synthesized (AgNPs). The effective production of AgNPs was supported by the results of Various characterization methods including TEM<sup>+</sup>, DLS, and UVVis. Synthesized AgNPs also abrogated the viability of ovarian cancer cells mainly by improving Bax/Bcl-2 ratio and also up-regulating caspase 3 and caspase 8.

#### REFERENCES

- Gamboa, S.M., et al., Synthesis and characterization of silver nanoparticles and their application as an antibacterial

- agent. *Int. J. Biosen. Bioelectron*, 2019, 5: p. 166-173.
2. Kouhbanani, M.A.J., et al., Green Synthesis of Spherical Silver Nanoparticles Using *Ducrosia Anethifolia* Aqueous Extract and Its Antibacterial Activity. *Journal of Environmental Treatment Techniques*, 2019, 7(3): p. 461-466.
  3. Vaid, P., et al., Biogenic silver, gold and copper nanoparticles-A sustainable green chemistry approach for cancer therapy. *Sustainable Chemistry and Pharmacy*, 2020, 16: p. 100247.
  4. Biao, L., et al., Green synthesis, characterization and application of proanthocyanidins-functionalized gold nanoparticles. *Nanomaterials*, 2018, 8(1): p. 53.
  5. Jeyaraj, M., et al., Biogenic silver nanoparticles for cancer treatment: an experimental report. *Colloids and surfaces B: Biointerfaces*, 2013, 106: p. 86-92.
  6. Gurunathan, S., et al., Green synthesis of silver nanoparticles using *Ganoderma neo-japonicum* Imazeki: a potential cytotoxic agent against breast cancer cells. *International journal of nanomedicine*, 2013, 8: p. 4399.
  7. Kouhbanani, M.A.J., et al., One-step green synthesis and characterization of iron oxide nanoparticles using aqueous leaf extract of *Teucrium polium* and their catalytic application in dye degradation. *Advances in Natural Sciences: Nanoscience and Nanotechnology*, 2019, 10(1): p. 015007.
  8. Lee, K.X., et al., Recent developments in the facile bio-synthesis of gold nanoparticles (AuNPs) and their biomedical applications. *International journal of nanomedicine*, 2020, 15: p. 275.
  9. Lohrasbi, S., et al., Green Synthesis of Iron Nanoparticles Using *Plantago major* Leaf Extract and Their Application as a Catalyst for the Decolorization of Azo Dye. *BioNanoScience*, 2019, 9(2): p. 317-322.
  10. Beheshtkhou, N., et al., Green synthesis of iron oxide nanoparticles by aqueous leaf extract of *Daphne mezereum* as a novel dye removing material. *Applied Physics A*, 2018, 124(5): p. 1-7.
  11. Kouhbanani, M.A.J., et al., Green synthesis of iron oxide nanoparticles using *Artemisia vulgaris* leaf extract and their application as a heterogeneous Fenton-like catalyst for the degradation of methyl orange. *Materials Research Express*, 2018, 5(11): p. 115013.
  12. Mikhailova, E.O., Gold Nanoparticles: Biosynthesis and Potential of Biomedical Application. *Journal of Functional Biomaterials*, 2021, 12(4): p. 70.
  13. Khan, S.H., Green nanotechnology for the environment and sustainable development, in *Green materials for wastewater treatment*. 2020, Springer. p. 13-46.
  14. Kouhbanani, M.A.J., et al., Green Synthesis and Characterization of Spherical Structure Silver Nanoparticles Using Wheatgrass Extract. *Journal of Environmental Treatment Techniques*, 2019, 7(1): p. 142-149.
  15. Jadoun, S., et al., Green synthesis of nanoparticles using plant extracts: A review. *Environmental Chemistry Letters*, 2021, 19(1): p. 355-374.
  16. Singh, M.P., et al., Biogenic and non-biogenic waste utilization in the synthesis of 2D materials (graphene, h-BN, g-C2N) and their applications. *Frontiers in Nanotechnology*, 2021: p. 53.
  17. Mousavi, B., F. Tafvizi, and S. Zaker Bostanabad, Green synthesis of silver nanoparticles using *Artemisia turcomanica* leaf extract and the study of anti-cancer effect and apoptosis induction on gastric cancer cell line (AGS). *Artificial cells, nanomedicine, and biotechnology*, 2018, 46(sup1): p. 499-510.
  18. Gasparetto, J.C., et al., Ethnobotanical and scientific aspects of *Malva sylvestris* L.: a millennial herbal medicine. *Journal of Pharmacy and Pharmacology*, 2012, 64(2): p. 172-189.
  19. Mousavi, S.M., et al., A Review on Health Benefits of *Malva sylvestris* L. Nutritional Compounds for Metabolites, Antioxidants, and Anti-Inflammatory, Anticancer, and Antimicrobial Applications. *Evidence-Based Complementary and Alternative Medicine*, 2021, 2021.
  20. Mravčáková, D., et al., Effect of *Artemisia absinthium* and *Malva sylvestris* on Antioxidant Parameters and Abomasal Histopathology in Lambs Experimentally Infected with *Haemonchus contortus*. *Animals*, 2021, 11(2): p. 462.
  21. Mosleh-Shirazi, S., et al., Biosynthesis, simulation, and characterization of Ag/AgFeO<sub>2</sub> core-shell nanocomposites for antimicrobial applications. *Applied Physics A*, 2021, 127(11): p. 1-8.
  22. Gopinath, P., et al., Implications of silver nanoparticle induced cell apoptosis for in vitro gene therapy. *Nanotechnology*, 2008, 19(7): p. 075104.
  23. Ahmadian, E., et al., Effect of silver nanoparticles in the induction of apoptosis on human hepatocellular carcinoma (HepG2) cell line. *Materials Science and Engineering: C*, 2018, 93: p. 465-471.
  24. Foldbjerg, R., D.A. Dang, and H. Autrup, Cytotoxicity and genotoxicity of silver nanoparticles in the human lung cancer cell line, A549. *Archives of Toxicology*, 2011, 85(7): p. 743-750.
  25. Syed, A., et al., Biological synthesis of silver nanoparticles using the fungus *Humicola* sp. and evaluation of their cytotoxicity using normal and cancer cell lines. *Spectrochimica Acta Part A: Molecular and Biomolecular Spectroscopy*, 2013, 114: p. 144-147.
  27. Rohini, B., et al., AgNPs from *Nigella sativa* Control Breast Cancer: An In Vitro Study. *J Environ Pathol Toxicol Oncol*, 2019, 38(2): p. 185-194.
  28. Singh, S.P., et al., Silver Nanoparticles Synthesized Using *Carica papaya* Leaf Extract (AgNPs-PLE) Causes Cell Cycle Arrest and Apoptosis in Human Prostate (DU145) Cancer Cells. *Biol Trace Elem Res*, 2021, 199(4): p. 1316-1331.
  29. Baharara, J., et al., Silver nanoparticles biosynthesized using *Achillea biebersteinii* flower extract: apoptosis induction in MCF-7 cells via caspase activation and regulation of Bax and Bcl-2 gene expression. *Molecules*, 2015, 20(2): p. 2693-2706.
  30. Kavya, J., et al., Silver nanoparticles induced lowering of BCL2/Bax causes Dalton's Lymphoma tumour cell death in mice. *Journal of Bionanoscience*, 2013, 7(3): p. 276-281.
  31. Khan, M.S., et al., Anticancer Potential of Biogenic Silver Nanoparticles: A Mechanistic Study. *Pharmaceutics*, 2021, 13(5).
  32. Zhang, X.-F. and S. Gurunathan, Combination of salinomycin and silver nanoparticles enhances apoptosis and autophagy in human ovarian cancer cells: an effective anticancer therapy. *International journal of nanomedicine*, 2016, 11: p. 3655.
  33. Fard, N.N., et al., Biogenic synthesis of AgNPs using *Artemisia oliveriana* extract and their biological activities for an effective treatment of lung cancer. *Artif Cells Nanomed Biotechnol*, 2018, 46(sup3): p. S1047-s1058.